

PAPER • OPEN ACCESS

## Calculation of ionized chemically nonequilibrium flow around a reentry module

To cite this article: A M Molchanov and V E Popov 2019 *J. Phys.: Conf. Ser.* **1370** 012013

View the [article online](#) for updates and enhancements.



**IOP | ebooks™**

Bringing you innovative digital publishing with leading voices to create your essential collection of books in STEM research.

Start exploring the [collection](#) - download the first chapter of every title for free.

# Calculation of ionized chemically nonequilibrium flow around a reentry module

A M Molchanov<sup>1</sup> and V E Popov<sup>1</sup>

<sup>1</sup> Moscow Aviation Institute (National Research University) ,  
Russia, 125993 Moscow, Volokolamskoe shosse, 4

vario999@mail.ru

**Abstract.** A method for calculating a hypersonic ionized flow at the entrance of the reentry module into the Earth's atmosphere has been developed. The mathematical modeling of such a flow was performed using a system of equations, which includes the equations of the continuity of components, the equation of momentum, the equations of total energy, vibrational energy, and electron energy. Chemical reactions and ionization reactions were taken into account. The vibrational temperatures of diatomic molecules and electrons were calculated. Calculations were made for various flight altitudes (60-85 km) at free-stream speeds from the first to the second cosmic velocity. The results of computations according to the proposed methodology are in satisfactory agreement with the experimental data and the computation results of other authors.

## 1. Introduction

The relevance of this work is due to the need for the most accurate prediction of the parameters of heat and mass transfer on the surface of aircraft by a chemically nonequilibrium ionized flow at the design stage. The correct solution to this problem allows us to optimize its trajectory, geometric, weight and layout parameters; and, accordingly, determine the requirements for the necessary thermal protection of the device already at the development stage of the image. For aircraft, it is especially important to determine the thermal conditions of such most heat-stressed surface areas as the toe of the fuselage, the front edges of the wings, the edges of the input devices, etc. As a rule, these elements in aircraft have the form of blunted bodies. Therefore, a sphere was chosen as a body to study.

## 2. Mathematical model

### 2.1. Basic equations describing the flow of an ionized gas mixture

The flow is modeled assuming that the continuum approximation is valid. It is assumed that the rotational and translational energy modes of all species can be described by a single temperature  $T_{tr}$  because the rotational energy equilibrates with the translational energy in just a few collisions [1]:

$$\frac{\partial \mathbf{U}}{\partial t} + \frac{\partial}{\partial x} (\mathbf{E}_c - \mathbf{E}_v) + \frac{\partial}{\partial y} (\mathbf{F}_c - \mathbf{F}_v) + \frac{\partial}{\partial z} (\mathbf{G}_c - \mathbf{G}_v) = \mathbf{S} , \quad (1)$$

Where variables  $\mathbf{U}, \mathbf{E}_c, \mathbf{E}_v, \mathbf{F}_c, \mathbf{F}_v, \mathbf{G}_c, \mathbf{G}_v, \mathbf{S}$  refer to article [8].



## 2.2. Thermodynamic Properties

The total energy contained in a unit volume consists of the internal energy and the kinetic energy of the gas mixture. Accordingly, the internal energy includes translational, rotational, vibrational, electronic and chemical components. Thus,

$$\rho E = \sum_{s \neq e}^{Nc} \rho_s c_{v,s} T + \sum_m^{Nm} \rho E_{v,m} + \rho E_e + \sum_s^{Nc} \rho_s h_s^0 + \frac{1}{2} \sum_{s \neq e}^{Nc} \rho_s u_i u_i \quad (2)$$

Here:  $\rho_s$  is the density of species  $s$ ;  $c_{v,s}$  is translational-rotational heat capacity at constant volume;  $T$  is translational-rotational temperature;  $h_s^0$  is the heat of formation of species  $s$ .

Pressure is the sum of partial pressures:

$$p = \sum_{s \neq e} \rho_s \frac{R}{M_s} T + p_e \quad (3)$$

where  $M_s$  is the molar mass of species  $s$ ;  $R$  is the universal gas constant.

The equations of state for electrons:

$$E_e = C_e \frac{3}{2} \frac{R}{M_e} T_e, \quad p_e = \rho_e \frac{R}{M_e} T_e \quad (4)$$

Here, the following assumptions were used: the electron dynamic pressure can be neglected and the excited electron states of molecules are negligible relative to the energies contained in other modes.

For the vibrational energy, we used an approach based on the model of a harmonic oscillator, according to which the average number of the  $m$ -th vibrational quanta  $\alpha_m$  per one molecule is determined by the formula

$$\alpha_m = r_m \frac{1}{\exp(\theta_m / T_{v,m}) - 1} \quad (5)$$

where  $\theta_m$  is the characteristic vibrational temperature of the  $m$ -th vibrational mode;  $T_{v,m}$  is appropriate vibrational temperature;  $r_m$  is the degree of degeneracy of the  $m$ -th mode of the molecule.

The specific (per unit mass of the component to which this mode belongs) vibrational energy of the  $m$ -th vibrational mode  $e_{v,m}$  is related to  $\alpha_m$  as following:

$$e_{v,m} = \frac{R\theta_m}{M_{s(m)}} \alpha_m = \frac{r_m \theta_m (R / M_{s(m)})}{\exp(\theta_m / T_{v,m}) - 1} \quad (6)$$

where  $M_{s(m)}$  is the molar mass of the species  $s$  to which the  $m$ -th vibrational mode belongs.

## 2.3. Viscous Terms

For the viscous stress tensor, the following formula is used

$$\tau_{ij} = \mu \left[ \frac{\partial u_j}{\partial x_i} + \frac{\partial u_i}{\partial x_j} \right] - \frac{2}{3} \mu \delta_{ij} \frac{\partial u_m}{\partial x_m}, \quad (7)$$

$\mu$  is the coefficient of dynamic viscosity.

Heat fluxes:

$$q_j = -\frac{\mu}{Pr} \frac{\partial h}{\partial x_j}, \quad q_{v,m,j} = -\frac{\mu}{Pr} \frac{\partial E_{v,m}}{\partial x_j}, \quad q_{e,j} = -\frac{\mu}{Pr} \frac{\partial h_e}{\partial x_j} \quad (8)$$

where  $h$ ,  $h_e$  are the enthalpies of the gas mixture and electrons, respectively:

$$h_e = E_e + \frac{P_e}{\rho} \quad (9)$$

When deriving the formulas (8), the assumption of similarity of heat transfer and diffusion was used, i.e. the equality of Schmidt and Prandtl numbers ( $Sc=Pr$ ).

The diffusion fluxes are modeled using Fick's law modified to enforce that the sum of the diffusion fluxes is zero:

$$\mathbf{g}_{s \neq e} = \mathbf{J}_s - C_s \sum_{r \neq e} \mathbf{J}_r, \quad \mathbf{J}_s = -\rho D_s \nabla C_s \quad (10)$$

The diffusion flux of electrons is calculated assuming ambipolar diffusion to guarantee the charge neutrality of the flow field by

$$\mathbf{g}_e = M_e \sum_{s \neq e} \frac{\mathbf{g}_s Q_s}{M_s} \quad (11)$$

where  $Q_s$  is the species charge.

#### 2.4. Transport Properties

The viscosity of the mixture is calculated by [2]

$$\mu = \sum_{s \neq e} \frac{m_s \gamma_s}{\sum_{r \neq e} \gamma_r \Delta_{sr}^{(2)}(T) + \gamma_e \Delta_{se}^{(2)}(T_e)} + \frac{m_e \gamma_e}{\sum_r \gamma_r \Delta_{er}^{(2)}(T_e)} \quad (12)$$

where

$$\gamma_s = \frac{\rho_s}{\rho M_s} \quad (13)$$

$m_s$  - is the mass of each species molecule or atom.

The binary diffusion coefficients between all particles except electrons are calculated by [2]

$$D_{sr} = \frac{k_B T}{p \Delta_{sr}^{(1)}(T)} \quad (14)$$

and for electrons as

$$D_{er} = \frac{k_B T_e}{p \Delta_{er}^{(1)}(T_e)} \quad (15)$$

The species diffusion coefficient in Eq. (10) is given by

$$D_s = \frac{\gamma_t^2 M_s (1 - M_s \gamma_s)}{\sum_{r \neq s} (\gamma_r / D_{sr})}, \quad \gamma_t = \sum_s \gamma_s \quad (16)$$

The collision terms are given by

$$\Delta_{sr}^{(1)}(T) = \frac{8}{3} \left[ \frac{2M_s M_r}{\pi R T (M_s + M_r)} \right]^{1/2} 10^{-20} \pi \Omega_{sr}^{(1,1)}(T) \quad (17)$$

$$\Delta_{sr}^{(2)}(T) = \frac{16}{5} \left[ \frac{2M_s M_r}{\pi R T (M_s + M_r)} \right]^{1/2} 10^{-20} \pi \Omega_{sr}^{(2,2)}(T) \quad (18)$$

Here:  $\pi \Omega_{ij}^{(1,1)}$  is diffusion collision integral;  $k_B$  is the Boltzmann constant.

The constant  $10^{-20}$  converts the square Angstroms into square meters, which is the standard unit for collision integrals. The recommended values of collision integrals  $\Omega_{sr}^{(1,1)}, \Omega_{sr}^{(2,2)}$  for the interactions involving neutrals are taken from Wright et al. [3].

For electron-ion, ion-ion and electron-electron collisions the interaction potential can be modeled using shielded Coulomb potentials [3]. The resulting collision integrals can be curve fit to

$$\Omega^{(n,n)} = 5.0 \times 10^{15} \left( \lambda_D / T^* \right)^2 \ln \left\{ D_n T^* \left[ 1 - C_n \exp(-c_n T^*) \right] + 1 \right\} \quad (19)$$

where

$$\lambda_D = \sqrt{\frac{k_{B,CGS} T}{4\pi n_{e,CGS} e_{CGS}^2}}, \quad T^* = \frac{\lambda_D}{e_{CGS}^2 / (k_{B,CGS} T)}, \quad (20)$$

$k_{B,CGS}$  is the Boltzmann constant in CGS units,  $e_{CGS}^2$  is the fundamental charge in CGS units and  $n_{e,CGS}$  is the electron number density also in CGS units. The values for the coefficients  $D_n$ ,  $C_n$ ,  $c_n$  are taken from [3].

### 2.5. Energy Exchange Mechanisms

The source in the electron energy equation is

$$\rho \dot{E}_e = Q_{T-e} - \sum_m Q_{e-v,m} + \dot{w}_e e_e \quad (21)$$

where  $e_e = E_e / C_e = \frac{3}{2} \frac{R}{M_e} T_e$ ;  $Q_{T-e}$  is translation-electron (T-e) energy transfer rate;  $Q_{e-v,m}$  is electron-vibration energy transfer rate.

The source in the equation of the m-th vibrational energy is

$$\rho \dot{E}_{v,m} = Q_{T-v,m} + Q_{V-v,m} + Q_{e-v,m} - Q_{Rad-v,m} + \dot{w}_{s(m)} e_{v,m}, \quad (22)$$

where  $Q_{T-v,m}$  is translation-vibration (T-V) energy transfer rate;  $Q_{V-v,m}$  is vibrational-vibrational (V-V) energy transfer rate.

#### 2.5.1. Translational-electron transfer rate

For the T-e energy transfer rate the formula of Lee was used [4]:

$$Q_{T-e} = 3R\rho_e (T - T_e) \sqrt{\frac{8RT_e}{\pi M_e}} \sum_{r \neq e} \sigma_{er} \frac{\rho_r N_A}{M_r^2}, \quad (23)$$

where  $\sigma_{er}$  are cross sections of electron collisions with heavy particles;  $N_A$  is Avogadro number.

The collision cross sections of electrons with neutral particles were calculated on the basis of Yukikazu Itikawa's recommendations [5].

For the case of electron-ion interactions, the effective Coulomb cross section is given by [4]:

$$\sigma_{e,ions} = \frac{8\pi}{27} \left( \frac{\lambda_D}{T^*} \right)^2 \ln(1 + 9T^{*2}), \quad cm^2 \quad (24)$$

where Debye length is

$$\lambda_D = \sqrt{\frac{k_{B,CGS} T_e}{4\pi n_{e,CGS} e_{CGS}^2}}, \quad (25)$$

$$T^{*2} = \frac{\lambda_D^2}{e_{CGS}^4 / (k_{B,CGS} T_e)^2} = \frac{(k_{B,CGS} T_e)^3}{4\pi N_{e,CGS} e_{CGS}^6}, \quad (26)$$

#### 2.5.2. Electron-vibrational energy transfer rate

There is a significant exchange between the electron energy and the vibrational energy of molecular nitrogen. The exchange of the electron energy with the vibrational energy of other molecules is negligible. The Landau-Teller formula is used for the exchange of energy between the energy of electrons and the vibrational mode of nitrogen:

$$Q_{e-v,m} = \rho_{s(m)} \frac{M_{s(m)} e_{v,m}^* (T_e) - e_{v,m}}{M_e \tau_{em}}, \quad \text{for } s(m) = N_2 \quad (27)$$

where the relaxation time  $\tau_{em}$  is a function of electron temperature and pressure derived by Lee [6].

#### Translational-vibrational and vibrational-vibrational transfer rate

The mechanisms of (T-V) and (V-V) transitions are described in detail in [1].

#### 2.6. Chemical kinetics

The following system of chemical reactions is used for the calculation of high-enthalpy air flows

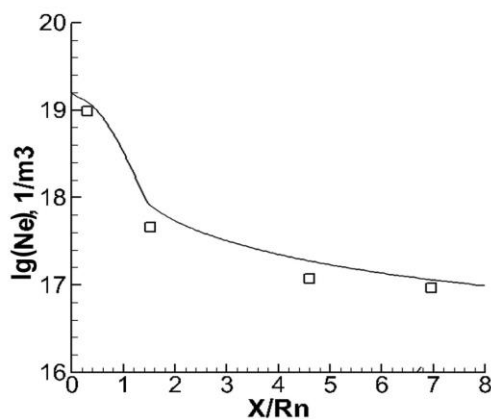


The details of determining reaction rates and component formation rates as a result of chemical reactions can be found in [1]. The forward and backward reaction rates are affected by the level of non-equilibrium in the flow. To account for that effect, Park's two-temperature model [7] is used. In that model the dissociation reactions are controlled by a combination of the translational-rotational and the vibrational temperature of the corresponding species

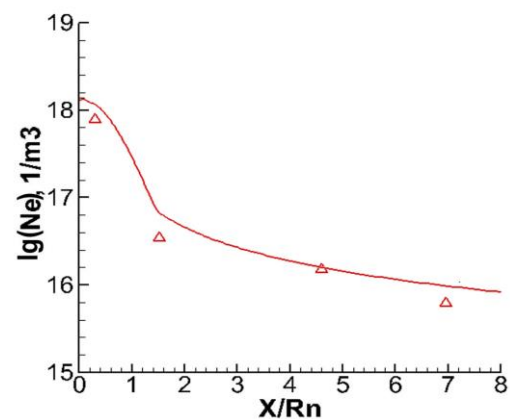
$$T_p = (T T_{v,m})^{1/2} \quad (28)$$

### 3. Results

The numerical method described in [8] was used for calculations.



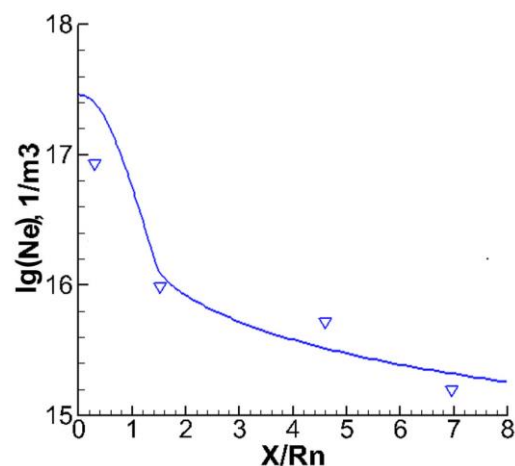
**Figure 1.** Comparison of peak electron number density at 72 km. Line - computation; Symbols - experiment [9].



**Figure 2.** Comparison of peak electron number density at 81 km. Line - computation; Symbols - experiment [9].

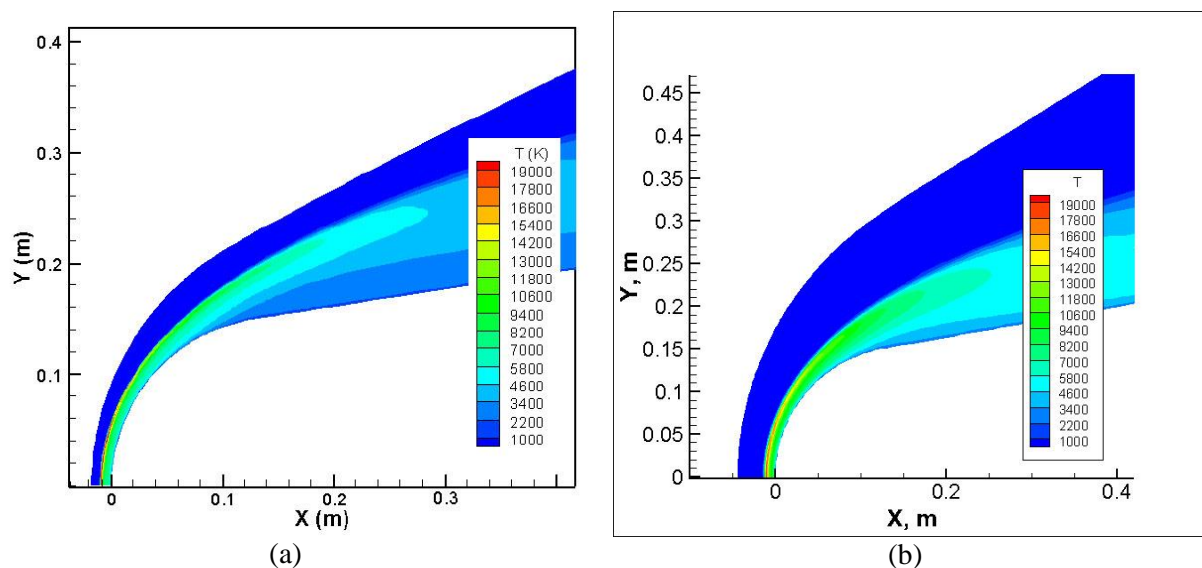
During the 1960s flight experiments [9] were conducted at high altitude, during which a vehicle was fired down through the atmosphere at hypersonic speeds. Measurements were made of electron densities at altitudes of 72,81,85 km. Figures 1-17 show the results from a numerical simulation of a flow past the sphere-cone shaped body, with nose radius 0.1524m, cone half-angle 9 degrees and body length 1.295m at different altitudes and at different flight velocities.

Figures 1-3 compare the computed results with the peak electron number density measured axially along the body at each altitude. The calculation results are compared with the experiment [9].



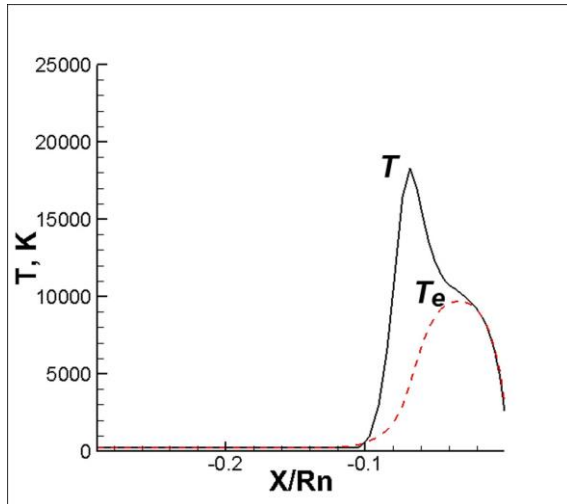
**Figure 3.** Comparison of peak electron number density at 85 km. Line - computation; Symbols - experiment [9].

Figure 4 shows a comparison of the results of calculating the temperature obtained by Scalabrin [10] with those obtained in this work.



**Figure 4.** Translational-rotational temperature countours at 71 km altitude. (a) computation of [10] ; (b) computation of this work

Translational-rotational and electron temperatures are shown along the stagnation streamline in Figures 5-9.



**Figure 5.** Temperatures on stagnation streamline at 72km, flight velocity = 7650 m/s

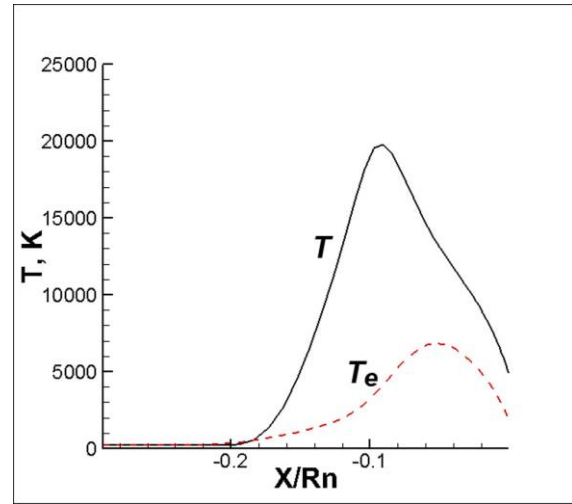


**Figure 6.** Temperatures on stagnation streamline at 81km, flight velocity = 7650 m/s

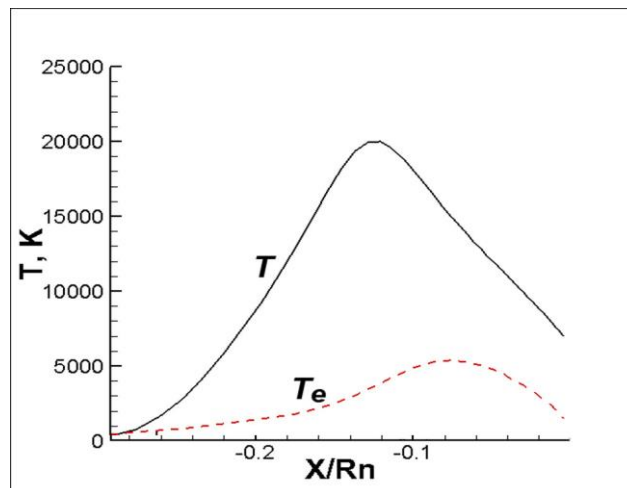


**Figure 7.** Temperatures on stagnation streamline at 85km, flight velocity = 7650 m/s

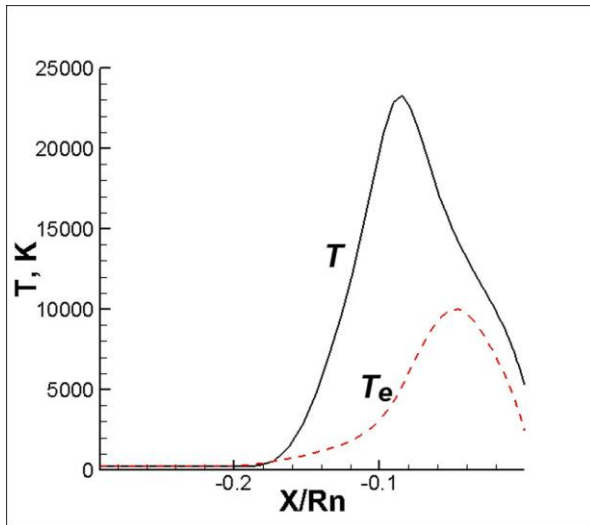


**Figure 8.** Temperatures on stagnation streamline at 81km, flight velocity = 8650 m/s

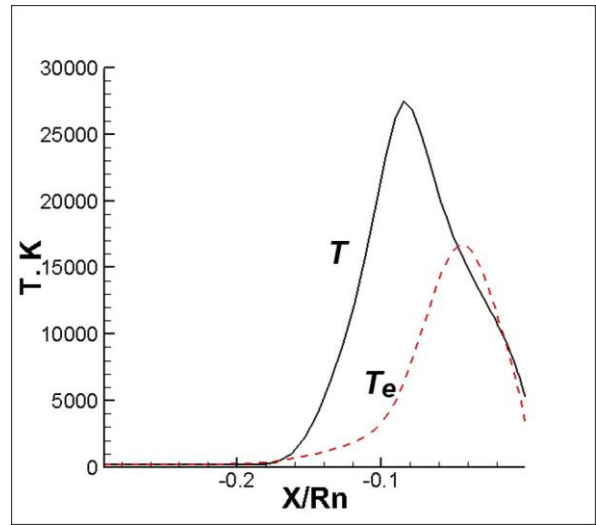


**Figure 9.** Temperatures on stagnation streamline at 81km, flight velocity = 9650 m/s

Mass fractions of species are shown along the stagnation streamline in Figures 10-15.

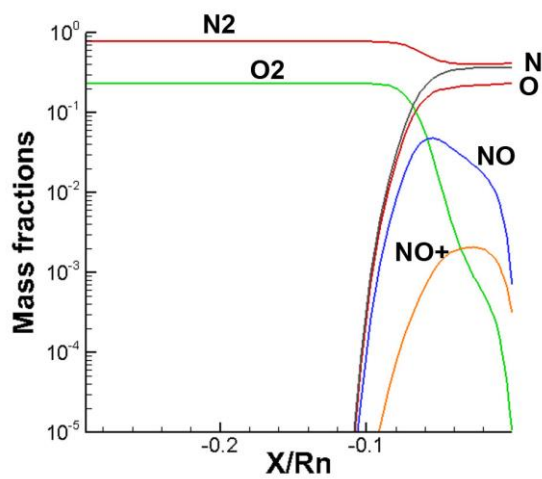


**Figure 10.** Mass fractions along stagnation streamline at 72km, flight velocity = 7650 m/s

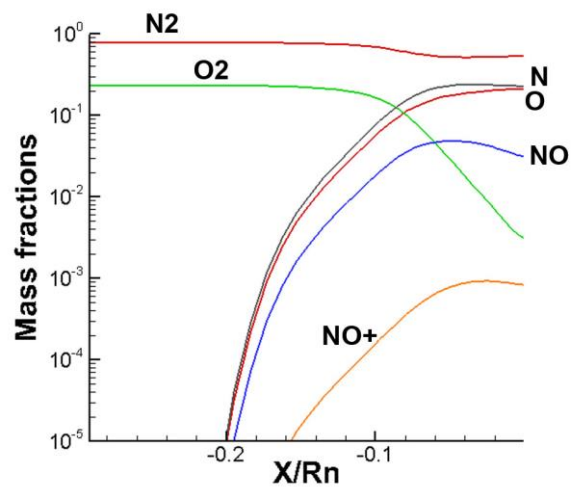


**Figure 11.** Mass fractions along stagnation streamline at 81km, flight velocity = 7650 m/s

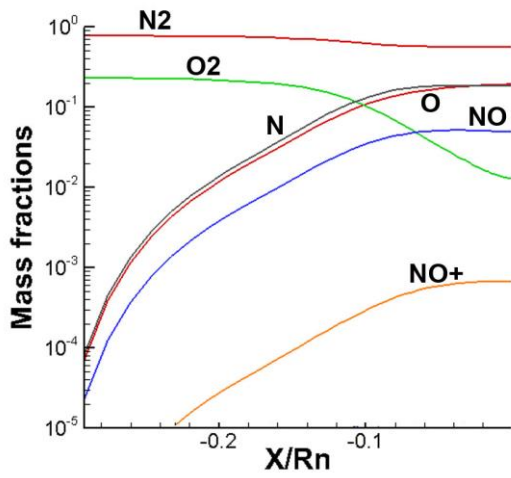


**Figure 12.** Mass fractions along stagnation streamline at 85km, flight velocity = 7650 m/s

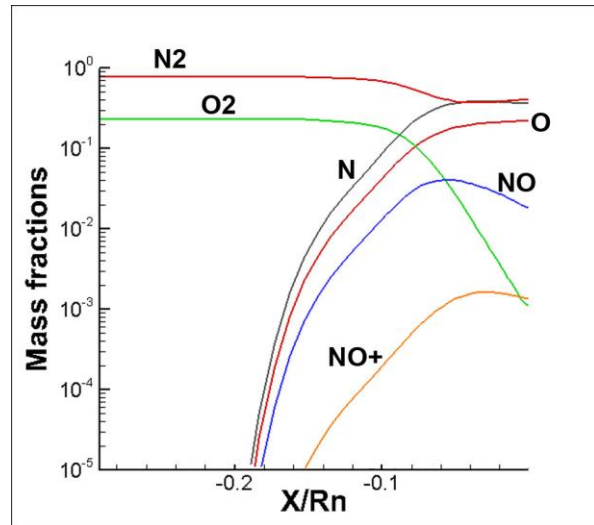


**Figure 13.** Mass fractions along stagnation streamline at 81km, flight velocity = 8650 m/s

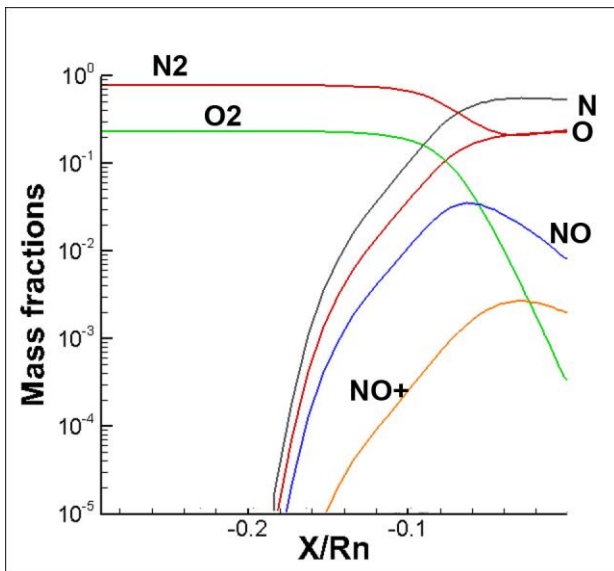


**Figure 14.** Mass fractions along stagnation streamline at 81km, flight velocity = 9650 m/s

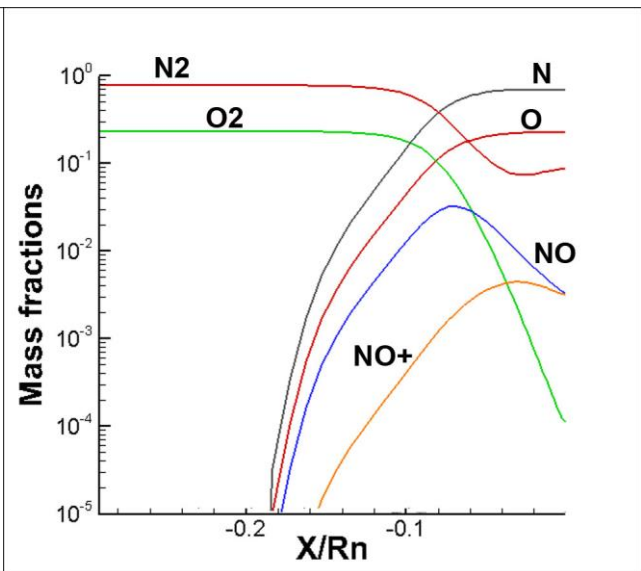


**Figure 15.** Mass fractions along stagnation streamline at 81km, flight velocity = 10650 m/s

Convective heat transfer rate under different flight conditions is presented in Figures 16-17.

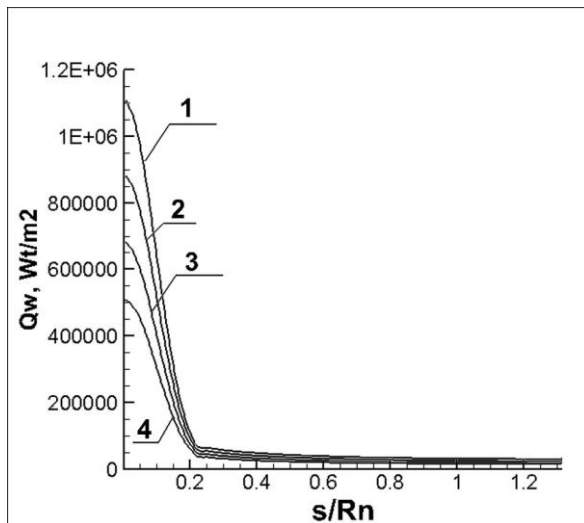


**Figure 16.** Convective heat transfer rate along the RAM-C II spacecraft at 81 km.

- 1 - flight velocity = 10650 m/s;
- 2 - flight velocity = 9650 m/s;
- 3 - flight velocity = 8650 m/s;
- 4 - flight velocity = 7650 m/s

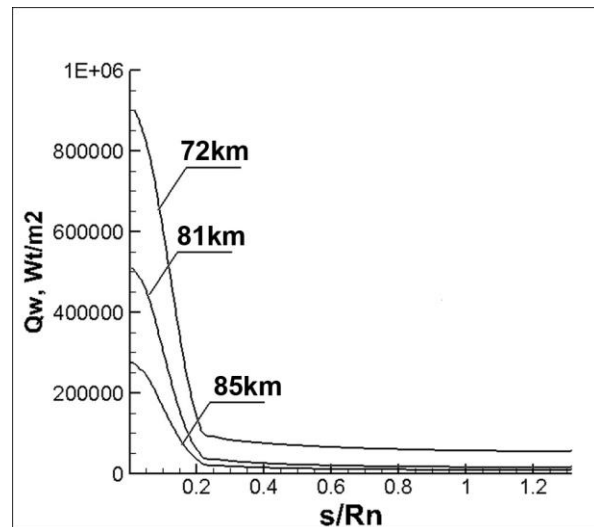


**Figure 17.** Convective heat transfer rate along the RAM-C II spacecraft at at different heights.

#### 4. Conclusions

A method for calculating a hypersonic ionized flow under conditions of thermochemical nonequilibrium has been developed. This flow is described by related partial differential equations for the conservation of mass, momentum, vibrational energy of each component, electron energy and total energy. A stable solution to these fully coupled equations was obtained for a gas consisting of seven chemical particles and characterized by six temperatures using an implicit method. The calculated electron number densities in the flow field of the spherical cone are in satisfactory agreement with the experimental data.

#### References

- [1] Molchanov A 2017 Mathematical modeling of hypersonic homogeneous and heterogeneous non-equilibrium flows in the presence of complex radiation-convective heat exchange. (Moscow, MAI) 159 p.
- [2] Gupta R, Yos J, Thompson R and Lee K 1990 NASA-RP-1232
- [3] Wright M, Bose D, Palmer G. and Levin E 2005 AIAA J. 43 2558
- [4] Lee J 1985 Progress in Aeronautics and Astronautics: Thermal-Design of Aeroassisted Orbital Transfer Vehicles 96, ed. H. F. Nelson (New York, AIAA) 3
- [5] Itikawa Y 2006 J. Phys. Chem. Ref. Data 35 31
- [6] Lee J 1986 Progress in Aeronautics and Astronautics: Thermophysical Aspects of Re-entry Flows 103, ed. J. N. Moss and C. D. Scott (New York, AIAA) 197
- [7] Park C 1990 Nonequilibrium Hypersonic Aerothermodynamics (New York, John Wiley & Sons)
- [8] Molchanov A AIAA Paper 2011-3211
- [9] Grantham W 1970 NASA TN D-6062
- [10] Scalabrin L 2007 Numerical Simulation of Weakly Ionized Hypersonic Flow over Reentry Capsules. Dissertation Abstracts International 68-10 6790